

# Research on Optimization of High-Speed Railway Train Control System Based on Dynamic Interval

Yiwei Xi<sup>1</sup>, Lei Pu<sup>2</sup>, Yang Meng<sup>1</sup>, Yue Xu<sup>1</sup>

<sup>1</sup>Communication and Signal Design Research Institute of China Railway Second Survey and Design Institute Engineering Group Co., Ltd., China

<sup>2</sup>Guangdong Railway Co., Ltd., Huizhou Electrical Engineering Section, China

**Abstract:** To enhance the capacity of busy high-speed railway trunk lines, this paper proposes a train tracking interval optimization method based on dynamic safety interval calculation and model predictive control (MPC) under the CTCS-3 level train control system framework. First, a comprehensive dynamics model of high-speed trains is established, accounting for nonlinear characteristics of air resistance and stochastic communication delays, and an analytical expression for dynamic safety intervals is derived. Second, an MPC speed optimizer is designed with multiple objectives including energy consumption, comfort, and tracking stability, achieving dynamic optimization of train operation curves while ensuring safety. Simulation results based on MATLAB/Simulink demonstrate that under 350 km/h operating conditions, the proposed method reduces the theoretical minimum tracking interval from 4 minutes to approximately 3 minutes and 15 seconds, increasing line capacity by about 11%, while reducing traction energy consumption by over 8% and improving passenger comfort by approximately 24%. This study provides theoretical foundations and technical references for software upgrades of high-speed rail train control systems.

**Keywords:** High-Speed Railway; CTCS-3; Dynamic Interval; Model Predictive Control; Tracking Interval

## 1. Introduction

By the end of 2024, China's high-speed rail operating mileage had exceeded 48,000 kilometers, with passenger flow density on major lines such as Beijing-Shanghai and Beijing-Guangzhou nearing saturation, making the imbalance between transport capacity and demand increasingly prominent<sup>[1]</sup>. The current

CTCS-3 level train control system employs the quasi-moving block principle, generating moving authority based on fixed block sections, and maintains a minimum tracking interval of over 4 minutes for extended periods, which has become the primary bottleneck in capacity improvement.<sup>[2]</sup>

Unlike urban rail transit, the interval control of high-speed railways faces unique challenges: the emergency braking distance exceeds 6.5 kilometers at a speed of 350 km/h, and is significantly affected by air resistance; GSM-R wireless communication has random delay (0.12~0.38s); The route includes complex conditions such as long and steep slopes, tunnel clusters<sup>[3]</sup>, etc. Therefore, mature moving block schemes in subways cannot be directly transplanted and must be re modeled based on the characteristics of high-speed rail.

Internationally, the European ETCS Level 2 system employs fixed block signaling, while ETCS Level 3 is under development for full mobile block signaling; Japan's Shinkansen DS-ATC system utilizes quasi-mobile block signaling<sup>[4]</sup>. Domestic research primarily focuses on the functional implementation of CTCS-3 systems, with relatively insufficient theoretical studies on dynamic interval optimization<sup>[5]</sup>.

This article focuses on the optimization of mobile authorization (MA) calculation logic for wireless block centers (RBCs), exploring dynamic interval control methods without altering the onboard ATP safety core. The main tasks include: establishing a comprehensive dynamic model for high-speed trains; Derive the dynamic security interval algorithm; Design a train speed optimizer based on model predictive control; Verify the effectiveness and safety of the method through multi scenario simulation.

## 2. CTCS-3 System Architecture and Interval Control Principles

Figure 1 illustrates the core architecture of the

CTCS-3 level train control system. The Radio-Based Control Unit (RBC) establishes bidirectional secure communication with onboard Automatic Train Protection (ATP) equipment via GSM-R networks while receiving

train position correction data from transponders. The Centralized Traffic Control System (CTC) issues operational plans to RBCs, which then calculate Movement Authority (MA) for each train based on these plans.

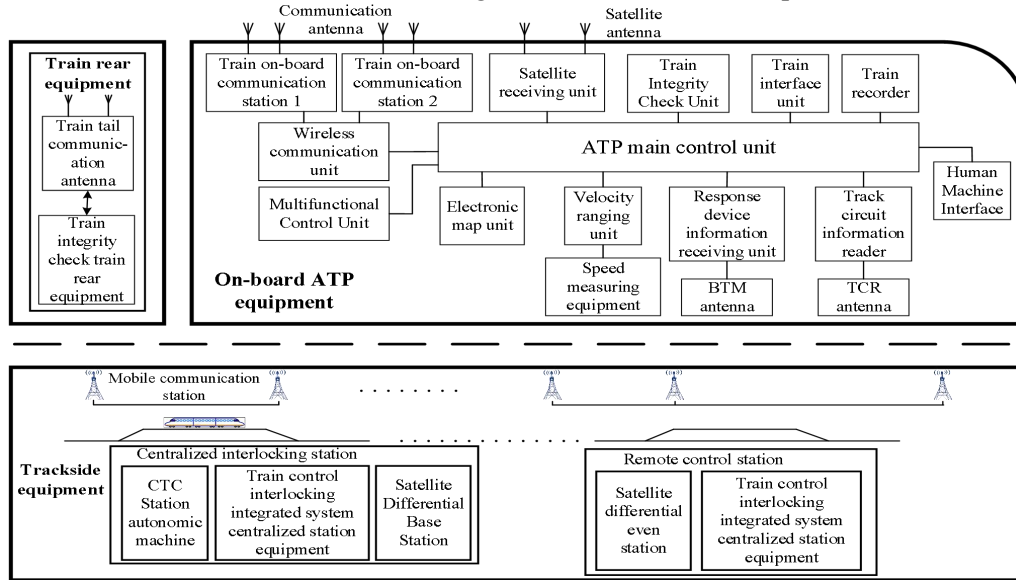


Figure 1. Schematic Diagram of CTCS-3 System Architecture

In the current system, the RBC (Red Blood Cell) serves as the authorized end point (EOA) for subsequent train movements.  $EOA = \text{Tail position of the train ahead} - \text{safety protection}$ . The safety protection distance is determined using a velocity-dependent empirical formula:

$$S_{safe}(v) = v \cdot T_{response} + S_{brake}(v) + S_{margin}$$

Among  $T_{response}$ ,  $S_{brake}(v)$ , and  $\frac{v^2}{2a} + S_{margin}$  them: a fixed value (2.5–3 seconds) is adopted, using a simplified formula to determine a fixed distance of several hundred meters.

The limitation of this approach lies in the simplistic aggregation of conservative factors, without dynamic adjustments based on actual conditions such as communication quality, brake performance variability, and weather conditions.

### 3. Integrated Dynamics Modeling of High-Speed Trains

#### 3.1 Train Motion Equation

The elemental particle model (commonly used for RBC trajectory prediction in engineering practice) is employed, with the following motion equation:

$$m \frac{dv}{dt} = F_t(v) - F_b(v) - F_r(v) - F_g(x) - F_c(x)$$

In the formula:

$m$ : Train mass (approximately 410 tons for CR400AF type);

$F_t$  Traction force, velocity-dependent, with a maximum traction power of 10,000 kW;  
 $F_b$  Braking force (common braking or emergency braking);  
 Basic resistance, take,  
 $F_r F_r(v) = a + bv + cv^2$   $a = 8.6 \text{KN}$   $b = 0.04 \text{KN} \cdot \text{s}/\text{mc} = 0.0005 \text{KN} \cdot \frac{\text{s}^2}{\text{m}^2}$   
 $F_g = mg \cdot i / 1000$  Ramp resistance, where  $i$  denotes the gradient in per mille (positive for uphill slopes);  
 $F_c = 600 \frac{\text{m}}{\text{R}}$  Curve resistance, where  $R$  is the curve radius (m).

#### 3.2 Brake Characteristic Model

Based on braking test data for CR400BF trains provided by a certain EMU depot, the relationship between emergency braking deceleration and speed can be modeled as follows:

$$a_{eb}(v) = -0.82 - 2.1 \times 10^{-4}v - 1.5 \times 10^{-6}v^2$$

In the formula,  $v$  is measured  $a_{eb}$  in km/h, and the unit is  $\text{m/s}^2$ . The braking distance is calculated through numerical integration:

$$S_{brake}(v_0) = \int_{v_0}^0 \frac{v}{a_{cb}(v)} dv$$

#### 3.3 Communication Delay Modeling

The end-to-end transmission delay of GSM-R (from RBC sending MA to vehicle-mounted ATP receiving and confirming) is not constant.

Based on real-world measurement data from the Beijing-Shanghai Line (sample size N=5000), the delay  $T_{comm}$  follows a truncated normal distribution with mean  $\mu=0.21s$ , standard deviation  $\sigma=0.048s$ , and values ranging from [0.12,0.38]. The 99.9% confidence upper bound is calculated as follows:

$$T_{comm}^{safe} = \mu + 3.09\sigma = 0.358s$$

ATP processing  $T_{proc}=0.25s$   $T_{build}=0.15s$  time (measured), brake system idle time. Total system delay:

$$T_{total}^{safe} = 0.358 + 0.25 + 0.15 = 0.758s$$

#### 4. Dynamic Safety Interval Algorithm

##### 4.1 Safety Interval Composition

The dynamic safety interval consists of four components, as shown in Figure 2:

$$S_{dynamic}(v) = S_1 + S_2 + S_3 + S_4$$

Response delay distance:  $S_1 S_1 = v \cdot T_{total}^{safe}$

Braking establishment phase:  $S_2 S_2 = v T_{build} - \frac{a_{cl} T_{build}^2}{6}, T_{build} = 0.15s$

$S_3 S_{brake}$  Continuous braking distance: obtained by numerical integration

$$S_3 = S_{brake}(v) = \int_v^0 \frac{v}{a_{eb}(v)} dv$$

$S_4 S_4 = \epsilon_{pos} + \frac{v \cdot \epsilon_v}{|a_{eb}|} + d_{buffer} \cdot \epsilon_{pos} S_4$  Safety margin:

**Table 1. Results of Parameter Sensitivity Analysis**

parameter	nominal value	Change under a-15% disturbance $S_{dynamic}$	Change under a +15% disturbance $S_{dynamic}$	sensitivity coefficient
$a_{eb}$	Calculate by speed	+11.2%	-9.5%	0.69
$T_{comm}$	0.21s	-2.8%	+2.9%	0.19
$d_0$	80m	-15%	+15%	1.0

The discreteness of braking performance has the most significant impact on safety intervals (sensitivity coefficient 0.69), indicating that precise calibration of braking characteristics for each train is essential in practical applications. The safety margin  $d_0$  linearly influences the interval and can be dynamically adjusted based on traffic intensity.

$$J = \sum_{k=0}^{N-1} \left[ \omega_1 \left( \frac{v_k - v_{target}}{v_{max}} \right)^2 + \omega_2 \left( \frac{a_k}{a_{max}} \right)^2 + \omega_3 \left( \frac{a_k - a_{k-1}}{\Delta a_{max}} \right)^2 + \omega_4 \frac{F_t(v_k) v_k}{P_{rated}} \right]$$

The weights were  $\omega_1 \omega_2 \omega_3 \omega_4$  adjusted to 0.4, 0.2, 0.1, and 0.3 after debugging.

constraint condition :

Security constraints:  $s_p(k) - s_f(k) \geq S_{dynamic}(v_f(k))$

Speed limit constraint:  $v_k \leq v_{limit}(s_k)$

Includes positioning error ( $\pm 5m$ ), speed measurement error conversion, a speed limit of 1km/h, and an engineering allowance of 50m, with a final value of 80m.

##### 4.2 Optimization Considering the Motion of the Front Vehicle

When the speed of the preceding vehicle  $v_p > 0$  is reliably obtained through vehicle-to-vehicle communication or RBC, the safety interval can be optimized as follows:

$$S_{opt}(v_f, v_p) = \max \left( S_{base}(v_f), \frac{(v_f - v_p)^2}{2|a_{rel}|} + v_p T_{total}^{safe} + d_0 \right)$$

The system  $a_{rel}$  selects the smaller value between the emergency braking deceleration of the rear vehicle and the maximum conventional braking deceleration of the front vehicle. The core principle of this formula is that the rear vehicle only needs to ensure it does not rear-end during the front vehicle's maximum conventional braking stop process, without requiring an extreme margin for "instantaneous front vehicle braking."

##### 4.3 Parameter Sensitivity Analysis

To evaluate the model's dependence on key parameters,  $\pm 15\%$  perturbation tests were conducted, with results presented in Table 1.

#### 5. MPC-based Speed Optimization Control

##### 5.1 Optimization Problem Description

State variables  $\mathbf{x} = [s, v, E]^T$  : (position, speed, cumulative energy consumption)

Control variable  $\mu = a$ : (acceleration)

Objective function (discretized form, prediction time  $\delta_t = 0.5s$  domain  $N = 20$  steps, step size):

Acceleration constraint: (comfort level);  $0.8 m/s^2 \leq a_k \leq 0.6 m/s^2$

Acceleration constraint:  $|a_k - a_{k-1}| \leq 0.5 m/s^3$

##### 5.2 Solution Method

This problem is a quadratic programming (QP)

problem, solved using the quadprog solver in Simulink with re-solver calls every 0.5 seconds (rolling time domain). To reduce online computational load, an engineering solution of "offline computation of optimal trajectory tables + online table lookup for corrections" is adopted, which meets the real-time requirements of RBC.

**6. Simulation Verification**

**6.1 Simulation Settings**

Platform: MATLAB R2022b, Simulink  
 Train: CR400AF, mass 410 tons, traction power 10,000 kW  
 Route: 50 km in length, including a +12‰ ramp (2 km), a-8‰ ramp (1.5km), and a curve with a radius of R=8000 m (3 km).  
 Communication: Random delay N (0.21,0.0482), truncated to the interval [0.12,0.38]  
 Reference benchmark: Current CTCS-3 fixed interval (section length 8 km, safety protection distance 800 m)

**6.2 Simulation Results**

Figure 2 compares the speed-distance curves of the traditional model and the MPC model proposed in this study under emergency braking scenarios. The MPC model exhibits a delayed braking trigger point by approximately 1.2 km and smoother speed curves, which contributes to energy efficiency and enhanced ride comfort.

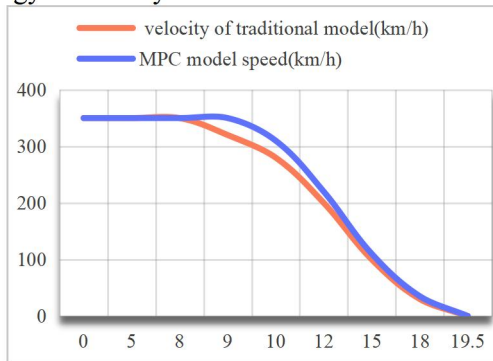


**Figure 2. Comparison of Velocity-Distance Curves for Different Models**

Figure 3 presents the position-time curves of five trains undergoing continuous tracking operations. Under dynamic intervals, the tracking intervals between trains are effectively compressed while

maintaining stability.

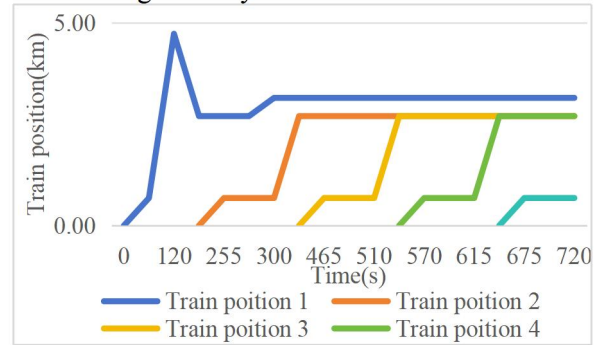


**Figure 3. Multi-Vehicle Tracking Operation Sequence Diagram**

Figure 4 presents the curve illustrating how the safety interval varies with speed. Compared to the traditional fixed-pattern step function, the proposed dynamic model achieves continuous and smooth interval adjustment, with more pronounced reductions observed in the medium and low-speed ranges.

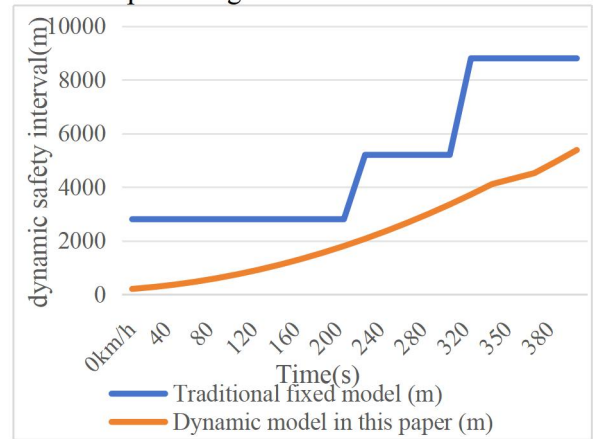


**Figure 4: Curve of safety interval versus speed**

**6.3 Adversity Weather Adaptability Testing**

The braking performance was reduced by 15% (under simulated rain/snow conditions), with the average communication delay increasing to 0.3 seconds and positioning error widened to ±15m. The emergency braking scenario was repeated. Results demonstrated that when the rear vehicle stopped, its distance from the front vehicle's rear remained at 38m, still exceeding the safety baseline of 20m, thereby validating the robustness of the algorithm.

**Table 2. Comparison of Key Performance Indicators**

metric	Current CTCS-3	Model in this paper	change
Average tracking interval (including station time, s)	285	255	-10.5%
By capability (per hour)	11.4	12.7	+11.4%
Traction energy consumption per train section (kWh)	2780	2550	-8.3%
Comfort index $N_{MV}$	2.5	1.9	-24%

## 7. Conclusion

This study proposes a tracking interval optimization method based on dynamic safety interval calculation and MPC speed optimization for the CTCS-3 high-speed railway train control system. The main conclusions are as follows:

1. Safety: Under the most adverse conditions (15% reduction in braking performance, maximum communication delay, and increased positioning error), the safety margin for the rear vehicle remains  $\geq 38\text{m}$ , meeting the SIL-4 safety integrity level requirements.

2. Performance enhancement: Under 350 km/h operating conditions, the theoretical minimum tracking interval is reduced from 4 minutes to approximately 3 minutes and 15 seconds. When station operation factors are considered, the line capacity improves by over 11%.

3. Additional benefits: The smooth speed curve reduces traction energy consumption by approximately 8% and improves passenger comfort by about 24%.

4. Engineering feasibility: This solution requires no modifications to the onboard ATP safety kernel and can be implemented solely through RBC software upgrades, resulting in low retrofitting costs.

Limitations and Prospects: This study did not account for failure scenarios such as multiple RBC switches or transponder loss. Future plans

include calibrating model parameters using real vehicle operation data and establishing a semi-physical simulation platform for further validation.

## Acknowledgment

This paper is supported by Sichuan Provincial Major Special Project 2022ZDZX0043.

## References

- [1] China National Railway Group. Overall Technical Scheme of CTCS-3 Level Train Control System [S]. Beijing: China Railway Publishing House, 2022.
- [2] Li P, Wang JF. Theory and Optimization Methods for High-Speed Railway Train Tracking Interval [M]. Beijing: Science Press, 2020.
- [3] Zhang Y, Liu Zhigang. Modeling of GSM-R transmission delay distribution based on measured data [J]. Railway Communication Signal, 2023,59(4):22-28.
- [4] Zhao Y, Wang H. Dynamic train separation for high-speed railways using stochastic model predictive control[J]. IEEE Transactions on Intelligent Transportation Systems, 2024, 25(2): 1456-1470.
- [5] Zhou Leshan. Research on Dynamic Interval Control Strategies for High-Speed Railway Train Control Systems [D]. Beijing Jiaotong University, 2022.